Chemical Science

ROYAL SOCIETY OF CHEMISTRY

REVIEW

View Article Online
View Journal | View Issue

Check for updates

Cite this: *Chem. Sci.*, 2022, **13**, 5069

Bioinspired superwettable electrodes towards electrochemical biosensing

Qinglin Zhu,[a] Yuemeng Yang,[a] Hongxiao Gao,[a] Li-Ping Xu *[a] and Shutao Wang *[b]

Superwettable materials have attracted much attention due to their fascinating properties and great promise in several fields. Recently, superwettable materials have injected new vitality into electrochemical biosensors. Superwettable electrodes exhibit unique advantages, including large electrochemical active areas, electrochemical dynamics acceleration, and optimized management of mass transfer. In this review, the electrochemical reaction process at electrode/electrolyte interfaces and some fundamental understanding of superwettable materials are discussed. Then progress in different electrodes has been summarized, including superhydrophilic, superhydrophobic, superaerophilic, superaerophobic, and superwettable micropatterned electrodes, electrodes with switchable wettabilities, and electrodes with Janus wettabilities. Moreover, we also discussed the development of superwettable materials for wearable electrochemical sensors. Finally, our perspective for future research is presented.

Received 31st January 2022
Accepted 22nd March 2022

DOI: 10.1039/d2sc00614f

rsc.li/chemical-science

Open Access Article. Published on 23 marec 2022. Downloaded on 19. 06. 2025 12:07:07.
This article is licensed under a Creative Commons Attribution-NonCommercial 3.0 Unported Licence.

Introduction

Billions of years of evolution endows many plants and animals with fascinating wetting properties to adapt to complex natural environments, such as the superhydrophobic lotus surface, underwater superoleophobic fish scales, or Nepenthes' slippery surface.[1–4] In the last two decades, much effort has been devoted to revealing the wetting behavior mechanism and fabricating artificial superwettable surfaces.[5–8] In 2021, superwettability was announced as one of the IUPAC Top Ten Emerging Technologies in Chemistry.[9] Superwettability has been employed in many applications, including self-cleaning, water harvesting, anti-icing, anti-fogging, anti-corrosion, printing, sensors, and water-oil separation.[10–18]

With the outbreak of coronavirus-2019, a massive number of diagnostic devices or biosensors are needed to fight this global pandemic. Innovation in biosensing technologies can accelerate the early diagnosis of diseases and the control of epidemics.[19] Recently, superwettable materials have injected new vitality into the construction of efficient biosensors.[20–26] Biosensing interfaces with special wettabilities exhibit unique solid–gas–liquid interfacial behavior and could further enhance the efficiency of biorecognition.[27] Special wettable materials have been broadly applied in biosensors and can be combined with different signal output methods, including fluorescence, electrochemistry, surface-enhanced Raman spectroscopy

[a]*Beijing Key Laboratory for Bioengineering and Sensing Technology, School of Chemistry and Biological Engineering, University of Science and Technology Beijing, Beijing 100083, P. R. China. E-mail: xuliping@ustb.edu.cn*

[b]*CAS Key Laboratory of Bio-inspired Materials and Interfacial Science, Technical Institute of Physics and Chemistry, Chinese Academy of Sciences, Beijing 100190, China. E-mail: stwang@mail.ipc.ac.cn*

Qinglin Zhu is currently a PhD student at the School of Chemistry and Biological Engineering, University of Science & Technology Beijing (USTB). He joined the Research Center for Bioengineering & Sensing Technology research group at USTB to pursue his PhD degree under the supervision of Prof. Li-Ping Xu. His study focuses on superwettable materials based biosensors and ultrasound driven nanomotors.

Yuemeng Yang is currently a PhD student at the School of Chemistry and Biological Engineering, University of Science & Technology Beijing (USTB). She joined the Research Center for Bioengineering & Sensing Technology research group at USTB to pursue her PhD degree under the supervision of Prof. Xueji Zhang and Prof. Li-Ping Xu. Her study focuses on superwettable microarrays for biosensing.

© 2022 The Author(s). Published by the Royal Society of Chemistry

Open Access Article. Published on 23 marec 2022. Downloaded on 19. 06. 2025 12:07:07.
This article is licensed under a Creative Commons Attribution-NonCommercial 3.0 Unported Licence.

(SERS), and colorimetry assay.[28–36] Among various biosensors, electrochemical biosensors have attracted extensive attention due to their high sensitivity, good selectivity, low cost, simple manipulation, multiplexed detection capabilities, ease of miniaturization, and real-time signal feedback.[37–39] The electrochemical sensing interface is crucial in electrochemical biosensors and directly affects the biosensing sensitivity, specificity, stability, and response dynamics.[40–45] Advantages that superwettable materials bring to electrochemical biosensors include, but are not limited to, behaving as biocompatible substrates for biomolecule immobilization, enlarging the active electrochemical areas, intelligent liquid management, favoring the enrichment of target biomolecules, and accelerating the desorption of products.[46–48] Most superwettable electrodes are nanostructured materials with high roughness, increasing the active electrode area dramatically. Superwettable surfaces also exhibit particular liquid management capability, which will play an important role in sample collection and multiplex biosensing. By optimizing the wettability of electrodes, the contacting behavior between reactants/products and electrodes can be varied, thus affecting the desorption/absorption of reactants or products.[49–51] Hence, the thermodynamics and reaction rates of electrochemical reactions can be well-tuned for improved performance of biosensors.

Inspired by natural superwettable interfaces, several superwettable electrodes have been fabricated, including superhydrophilic, superhydrophobic, superaerophilic, superaerophobic, superwettable patterned, Janus wettability, and wettability switchable electrodes as shown in Scheme 1.[51–57] Due to their remarkable features, these superwettable electrodes inject fresh energy into the development of electrochemical biosensing and exhibit outstanding promise.[58–60] Although superwettable electrodes are still in their infancy stage, it is required to summarize the progress in superwettable electrodes for sensitive and wearable biosensing and predict future studies in this field. First, we discussed the electrochemical reaction process at the electrode/electrolyte interfaces. Then, we introduced some fundamental understanding of superwettable materials. Subsequently, we summarized the recent progress of superwettable material-based electrochemical biosensors. Finally, we also highlighted the perspectives and challenges of superwettable electrodes. We expect this review to promote the further development of superwettable electrodes, intelligent electrochemical biosensors, and wearable biosensors towards routine disease surveillance or early diagnosis of malignant diseases.

Electrochemical reaction at the interfaces

Electrochemical sensing systems consist of a biorecognition element and a transducer. Biorecognition elements refer to the immobilized capture probes such as DNA, aptamer, antibodies, enzymes, or receptors.[40] Electrochemical transducer parts, *i.e.* electrodes, transfer the biorecognition process to the electrochemical signal. Electrochemical reactions are the core part of bioelectrochemical biosensors, occurring at an "electrified

Hongxiao Gao is currently a PhD student at the School of Chemistry and Biological Engineering, University of Science & Technology Beijing (USTB). She joined the Research Center for Bioengineering & Sensing Technology research group at USTB to pursue her PhD degree under the supervision of Prof. Li-Ping Xu. Her study focuses on patterned organohydrogel surface droplet arrays for biosensing.

Li-Ping Xu is a professor of chemistry at the Research Center for Bioengineering and Sensing Technology, University of Science & Technology Beijing. She obtained her PhD degree in physical chemistry from the Institute of Chemistry, Chinese Academy of Science, in July 2006. She was a postdoc fellow at the University of California, Santa Cruz from 2006–2007. Her research addresses problems at the interface of nanoscience, nanotechnology, and biotechnology, including the construction of novel functional nanomaterials and their applications in biosensors and biochips.

Shutao Wang is currently a Professor at the Technical Institute of Physics and Chemistry, Chinese Academy of Sciences TIPCCAS and University of Chinese Academy of Sciences. He received his PhD degree (2007) from the Institute of Chemistry, Chinese Academy of Science (ICCAS) under the supervision of Prof. Lei Jiang. Then he worked in the Department of Molecular and Medical Pharmacology and the California NanoSystem Institute at the University of California in Los Angeles as a postdoctoral researcher (2007–2010). He was appointed as a Professor at ICCAS (2010–2014). His research interests include the design and synthesis of bio-inspired interfacial materials with special adhesion and their application at bio–nanomaterial interfaces.

© 2022 The Author(s). Published by the Royal Society of Chemistry

Open Access Article. Published on 23 marec 2022. Downloaded on 19. 06. 2025 12:07:07.
This article is licensed under a Creative Commons Attribution-NonCommercial 3.0 Unported Licence.

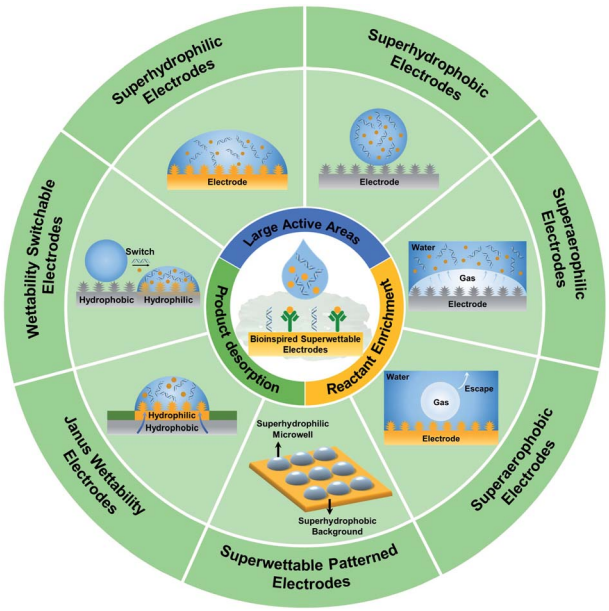

Scheme 1 Bioinspired superwettable surface for electrochemical biosensors. Due to their intrinsic advantages, including large active areas, intelligent liquid management, and dynamics acceleration, several superwettable materials have been applied in electrochemical biosensors. This review mainly focuses on the recent progress in superhydrophilic, superhydrophobic, superaerophilic, superwettable patterned, and Janus wettability electrodes, and electrodes with switchable wettability.

interface" between electrodes and electrolytes.[61,62] According to the Stern model, the electrode/electrolyte interfaces can be divided into the inner Helmholtz layer (IHP) filled with non-solvated ions, the outer Helmholtz layer (OHP) filled with solvated ions, and the diffuse layer where the ion diffusion occurs, as shown in Fig. 1a.[63,64] The electrochemical reaction generally occurs at the IHP.

In the electrochemical reaction, the reaction process is generally accompanied by reactant transport, product transport, and electron conduction, as shown in Fig. 1b.[65] For a reversible reaction, A + B ⇋ AB, the thermodynamics equilibrium constant can be defined as eqn (1),

$$K = \frac{C_{AB}}{C_A \times C_B} \quad (1)$$

where C is the concentration of the reactant and the product. K is constant under a given condition. Increasing the C_A or C_B or decreasing C_{AB} can promote the forward reaction. Enriching reactants or accelerating the desorption of products by changing the surface structure or interfacial properties can promote the forward reaction. Reactant enrichment and product escape can be realized by tailoring the wettability of electrodes, which will accelerate the thermodynamics of the electrochemical reaction.[59]

In addition to mass transfer, enhancing the current intensity is also crucial for improving the electrochemical sensitivity. The diffusion flux was employed further to explain the relationship between the current and interface reaction. In brief, the diffusion flux is the amount of substance that passes through a unit area in a unit of time, according to Fick's first law (eqn (2)),[66–68]

$$J = -D\frac{\partial C}{\partial x} \quad (2)$$

where J is the diffusion flux, D is the diffusion coefficient, C is the concentration of the component and x is the diffusion distance. Current is the amount of charge passing through any cross-section in unit time according to Faraday's law (eqn (3)),[69–72]

$$I = -JnFA = nFAD\frac{\partial C}{\partial x} \quad (3)$$

where I is the current, n is the reactant valence, F is the Faraday constant, and A is the electrode area. Generally, the reactant valence and Faraday constant are usually constant for a given

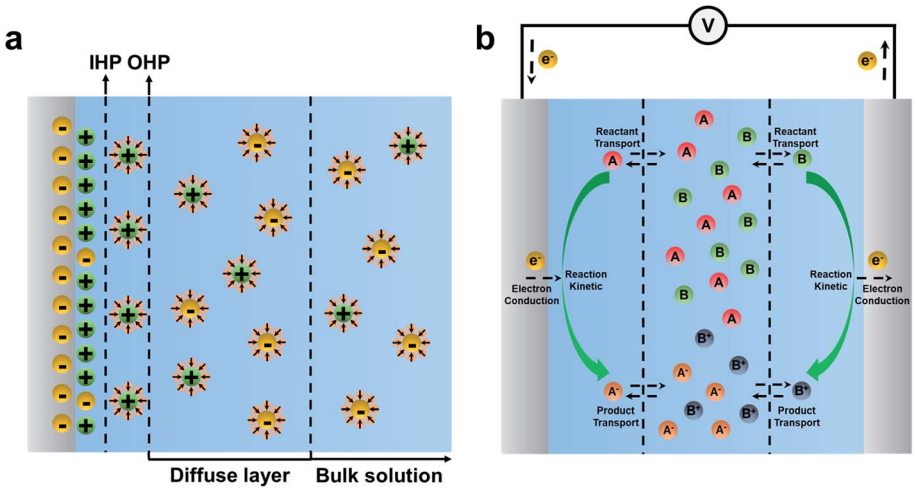

Fig. 1 Schematic illustration for the electrochemical reactions occurring at the interface between the electrode and electrolyte. (a) Stern model of the EDL generated on a negatively charged electrode surface. (b) The key processes consist of mass transport and electron conduction in an electrochemical reaction.

Open Access Article. Published on 23 marec 2022. Downloaded on 19. 06. 2025 12:07:07.
This article is licensed under a Creative Commons Attribution-NonCommercial 3.0 Unported Licence.

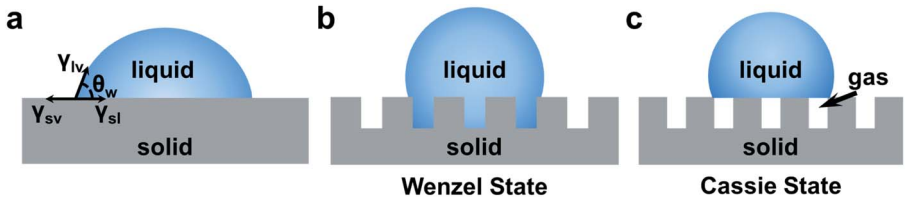

Fig. 2 (a) Definition of the contact angle of the droplet on an ideal surface. The wetting state on the rough surface: (b) Wenzel model and (c) Cassie model.

redox reaction. The current intensity is proportional to the diffusion flux and cross-sectional area. Thus, materials with high conductivity and a high surface area have a significant impact on the signal current. Most superwettable electrodes exhibit high roughness, which further favors the increase of current and improves the sensitivity of superwettable electrode-based biosensors.[73,74]

According to the above discussion, the development of electrodes that promote the enrichment of reactants, accelerate the desorption and escape of products, have high electrical conductivity, and high specific surface areas will facilitate the development of sensitive electrochemical biosensors.

General concepts about superwettable materials

Wettability generally refers to the liquid wetting ability on a solid surface. The wettability of the surface can be described using the contact angle (CA).[75] As shown in Fig. 2a, Young's equation described the relationship between the CA and interfacial energy on an ideal solid surface (smooth and chemically homogeneous surface) using eqn (4),[76]

$$\cos\theta_w = \gamma_{sv} - \gamma_{sl}/\gamma_{lv} \quad (4)$$

where θ_w is the CA of the liquid and γ_{sv}, γ_{sl}, and γ_{lv} are the specific energies of solid–vapor, solid–liquid, liquid–vapor, respectively. Young's equation revealed the relationship between wettability and surface energy. According to Young's equation, surfaces with special wettability can be constructed using a material with different surface energies.[77] The surface with a water CA less than 65° is hydrophilic, and the hydrophobic surface is the one with a water CA larger than 65°.[78,79] In particular, some surfaces have shown extreme wettability. Thus a further definition of superhydrophilic (CA < 5°) and superhydrophobic (CA > 150°) was proposed.[75,80] Surface wettability is determined by the surface chemical composition and morphology. Higher roughness of the surface can drive the wettability to the extreme.[6] Generally, two models, including the Wenzel and Cassie models, explain the wetting state on a rough surface. In the Wenzel model (Fig. 2b), the droplet was wetted into the surface structure at the contact area, resulting in high CA hysteresis.[81] In this case, the CA was enlarged by a factor r (related to the surface roughness) according to eqn (5).

$$\cos\theta_w^* = r\cos\theta_w \quad (5)$$

Eqn (5) shows that the surface roughness will promote either hydrophilicity or hydrophobicity of the surface. In the Cassie model (Fig. 2c), the droplet only sits on the top of the surface with a gas layer between the liquid and substrate, which leads to a liquid–gas–solid triphase interface.[82] In this composite state, the CA will be corrected by the area fraction (f_s) of the solid on the surface according to eqn (6).

$$\cos\theta_w^{**} = -1 + f_s(\cos\theta_w + 1) \quad (6)$$

As has been discussed, the wettability of the surface is determined by the chemical composition and roughness. For the fabrication of superwettable surfaces, high roughness nanostructures were constructed by different methods, including electrodeposition, self-assembly, etching, and so on. The modulation of the chemical composition can be achieved by direct use or chemical modification of materials with different surface energies. For the superwettable patterned

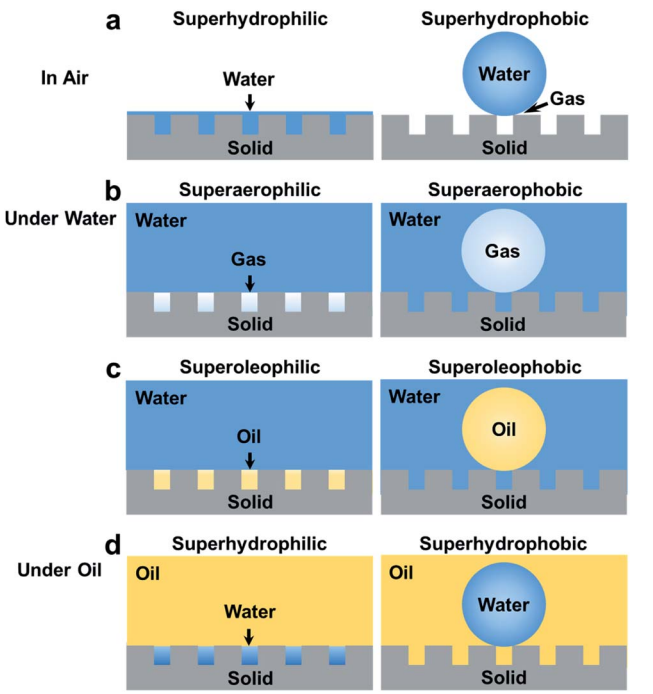

Fig. 3 The superwettability systems. (a) Superhydrophilicity (left) and superhydrophobicity states in air. (b) Underwater superaerophilicity (left) and superaerophobicity (right). (c) Underwater superoleophillicity (left) and superoleophobicity (right). (d) Underoil superhydrophilicity (left) and superhydrophobicity (right).

© 2022 The Author(s). Published by the Royal Society of Chemistry

Open Access Article. Published on 23 marec 2022. Downloaded on 19. 06. 2025 12:07:07.
This article is licensed under a Creative Commons Attribution-NonCommercial 3.0 Unported Licence.

surface, photoirradiation or plasma treatment through a photomask might be employed.

Recently, superwettable materials in air have been extended to water and oil systems. Several other types of superwettability are also studied, including underwater superaerophobicity, underwater superaerophilicity, underwater superoleophobicity, underwater superoleophilicity, underoil superhydrophilicity, underoil superhydrophilicity, *etc* as shown in Fig. 3.[14,77,83–86] Accordingly, the application of superwettable materials has also been extended.[87–91] Electrochemical reactions at superwettable electrodes may differ markedly from those on traditional electrodes due to the special interactions between solid, liquid, oil, and gas phases.[92,93] For example, the superoleophobic electrode can accelerate the desorption of oil phase products in the Kolbe reaction and greatly improve the working life of the electrode.[94] Highly efficient electrochemical biosensing can be achieved by tailoring the wettability of electrodes.

Superhydrophilic electrodes in electrochemical biosensing

Superhydrophilic surfaces with CA < 5° have high roughness and can be wetted by electrolyte solutions thoroughly according to the Wenzel model.[95] The Wenzel contact mode results in a large contact area between the electrolyte solution and the electrode, *i.e.*, higher electroactive surface areas, which improves the sensitivity for biochemical detection (Fig. 3a, left).[96] Metal electrodes have been broadly applied in electrochemical biosensors due to their excellent electrical conductivity and high surface energy. By fabricating hierarchical structures on metal electrodes, superhydrophilic electrodes with micro/nano roughness can be obtained. Compared with the planar electrode, the electrochemical sensing performance can be improved because of the increased specific surface area.[97]

Many superhydrophilic metal electrodes with rough structures have been constructed to detect proteins and nucleic acids. Our group has developed a superhydrophilic fractal gold electrode (FracAu) for electrochemical biosensors (Fig. 4a).[52,97] The superhydrophilic FracAu-based biosensor has been employed to detect thrombin and apolipoprotein E4 (APOE4) and achieved a limit of detection (LOD) of 5.7 fM for thrombin and 0.3 ng mL^{-1} for APOE4, respectively. Compared to the plain gold electrode, the LOD of the superhydrophilic FracAu electrode was reduced by 3 to 10 times, and the electroactive surface area was improved to almost 50 times. In addition, the fractal structure can decrease the steric hindrance, which can promote the bio-recognition efficiency between probes and targets. The FracAu electrode has provided a high sensitivity biosensor and shown great potential in detection. Besides, our group has developed a free-standing superhydrophilic Pt nanowire network electrode (PtNNE) for glucose biosensors (Fig. 4b).[73] The PtNNE exhibited high electrocatalytic activity and stability due to the 3D structure of high-index facet surface polycrystalline nanowires. The superhydrophilic PtNNE also provided an excellent sensitivity of 1360 μA mM^{-1} cm^{-2} for detecting hydrogen peroxide (H_2O_2) and 114 μA mM^{-1} cm^{-2} for detecting glucose. The excellent performance of the superhydrophilic PtNNE-based biosensor is ascribed to the 3D nanowire self-interconnecting network nanostructure induced

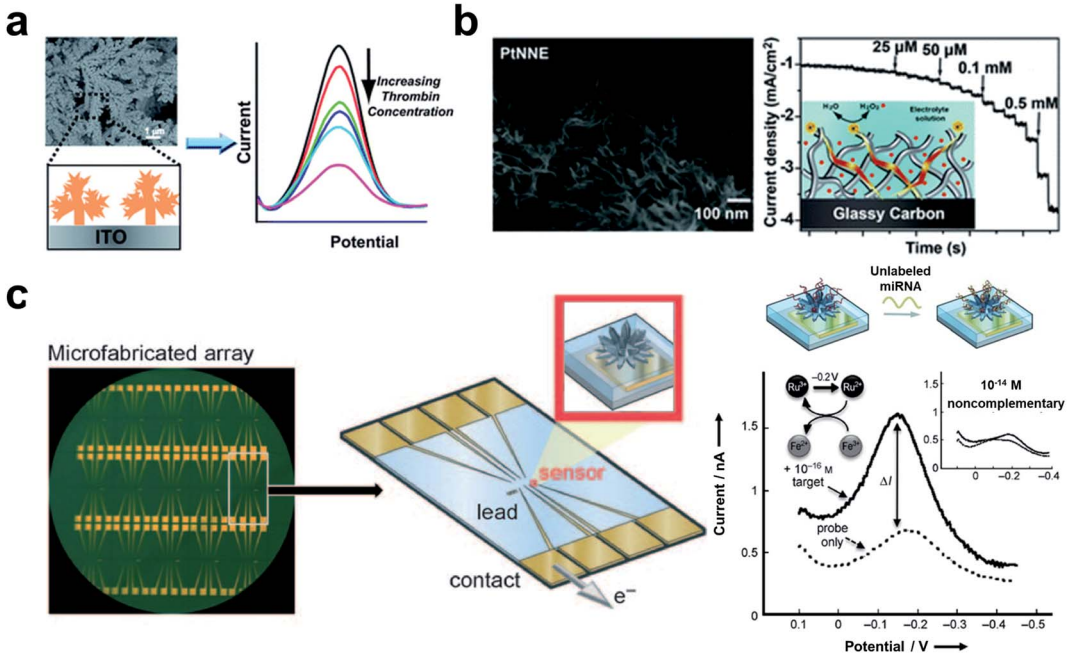

Fig. 4 The applications of superhydrophilic electrodes in biosensors. (a) The superhydrophilic fractal gold electrode for thrombin detection. Reproduced from ref. 52 with permission. Copyright 2012, Royal Society of Chemistry. (b) The superhydrophilic electrode based on the self-interconnecting Pt nanowire network for an electrochemical amperometric biosensor. Reproduced from ref. 73 with permission. Copyright 2015, Royal Society of Chemistry. (c) The NME array for the multiplexing miRNA detection. The signal of NME hybridized with target miRNA can be exported by differential pulse voltammetry (DPV). Adapted from ref. 101 with permission. Copyright 2009, Wiley-VCH.

Open Access Article. Published on 23 marec 2022. Downloaded on 19. 06. 2025 12:07:07.
This article is licensed under a Creative Commons Attribution-NonCommercial 3.0 Unported Licence.

high surface area and hydrophilicity. The electrochemical active surface area of PtNNE was measured as almost 214 times higher than that of the plane electrode. Moreover, the porous structure of PtNNE provided abundant active sites for rapid electron migration and mass transportation. On the other hand, the substrate-free noble metal electrode has shown better electrochemical properties than the substrate-based electrode. This superhydrophilic PtNNE has provided a reliable electrochemical platform for oxidase-based enzyme biosensors. Notably, the liquid wetting behavior on the superhydrophilic electrode is the Wenzel state, which makes the liquid thoroughly wet the electrode and further increases the sensitivity of the electrochemical biosensor.

Bulk superhydrophilic electrodes are generally used in large volumes of solutions, which causes large sample consumption. In addition, bulk superhydrophilic electrodes are not easily integrated into mobile biosensing platforms for portable biosensing. In this case, nanostructured microelectrodes (NMEs) with superhydrophilicity have attracted much attention due to their high electric current density, large specific surface area, and small size.[60,98] Microelectrodes are generally developed by electrochemical deposition. The as-prepared NMEs have a highly fractal nanostructure which further induces a superhydrophilic surface. Shana's group developed a Pd NME-based biosensor for the detection of nucleic.[99] PNA single strands were employed to capture the target with $[Ru(NH_3)_6]^{3+}$ and $[Fe(CN)_6]^{3-}$ as signal molecules. Due to the high surface area of the superhydrophilic nanostructured microelectrodes, the LOD of this nanostructured microelectrode-based biosensor is 1 fM, which is 100 times higher than that of a smooth microelectrode. Superhydrophilic NMEs lead to thorough wetting between the electrode and the electrolyte, increasing the sensitivity. The high curvature of NMEs causes lower steric hindrance, which is conducive to bioconjugation of the biomarkers.[100] Besides single biomarker detection, superhydrophilic NMEs have also shown great potential in the multiplex detection of biomarkers. Shana's group developed an NME array for multiplexing miRNA detection based on these nanostructured superhydrophilic microelectrodes, as shown in Fig. 4c.[101] The NME array was fabricated by electrodeposition of Pd on an Au micropatterned silicon substrate. The sensitive detection of miRNA was achieved with a LOD of 10 aM. Moreover, they have developed a gene-circuit-based sensor based on the NME array.[102] In response to the target, gene circuits generated restriction enzymes and released methylene blue-labeled reporter DNA. The capture DNA modified NMEs were then bioconjugated with the methylene blue-labeled reporter DNA for the output of the signal. The gene-circuit-based sensor has achieved sensitive and simultaneous detection of colistin antibiotic resistance genes (mcr-1, mcr-2, mcr-3, and mcr-4) with LOD of 1 fM for mcr-4. Such an approach has provided a multiplexing NME platform for electrochemical biosensors and shown great potential in high-throughput biosensing for clinical diagnoses. Besides, NMEs were combined with a neutralizer displacement assay (NDA) for simultaneous detection of nucleic, protein, and small molecules.[103] The neutralizer-modified NME exhibited a charge-free state. Displacement of the neutralizer in the presence of the target resulted in a change of charge which further generated an electrochemical signal. Such a NDA-based NME has achieved sensitive detection of cocaine, DNA (LOD 100 aM), *E.coli* RNA (10 pg mL^{-1}), bacteria (0.15 c.f.u. mL^{-1}), proteins (lower to 10 fM for thrombin), and adenosine triphosphate. And the NME-based neutralizer displacement assay has shown exciting multiplexing capabilities, which allows simultaneous detection of multiple analytes.

Nanostructured microelectrodes can also be combined with a digital microfluidic device to develop portable biosensors. Rackus *et al.* combined NMEs with digital microfluidics and achieved the sensitive rubella virus diagnosis with a LOD of 0.07 IU mL^{-1} for rubella virus IgG.[104] And digital microfluidics gives an alternative for automated manipulation sample handling as well as lowering sample consumption. Therefore, NME-based digital microfluidics has provided high-integration, automation, portable, user-friendly, and low-cost biosensors for distributed diagnoses (*e.g.* blood glucose meter) in practical applications.

According to the above discussion, superhydrophilic electrodes and superhydrophilic NMEs have provided high electrochemically active area and low steric hindrance in biosensors. And the incorporation of superhydrophilic electrodes with digital microfluidics has further provided an efficient approach for practical applications.

Superhydrophobic electrode in electrochemical biosensing

Inspired by the self-cleaning properties of lotus, many superhydrophobic surfaces have been developed and have various applications in different fields.[105] In electrochemical biosensing, the passivation of the electrode surface has led researchers to develop electrochemical biosensors. Superhydrophobic electrodes (CA > 150°) provide an optional solution for fabricating electrodes with long-term stability.[13] On the superhydrophobic electrode with a Cassie state, air was trapped between droplets and substrates, which led to a nonwet contact mode (Fig. 3a right). Superhydrophobic electrodes have exhibited particular self-cleaning properties and provided refreshable ability for repetitive use by simply washing. Zhu *et al.* developed a PDMS@MWCNT modified glassy carbon (GCE) superhydrophobic electrode for refreshable biosensors.[51] The polydimethylsiloxane (PDMS) provided a superhydrophobic surface, and the multi-walled carbon nanotubes (MWCNT) provided high conductivity. Due to the self-cleaning properties of the electrode, biosensors based on superhydrophobic electrodes have presented excellent stability in repeated experiments with a lower RSD (1.4% for dopamine and 5.5% for quercetin) of anodic peak current compared to the bare GCE (10.5% for dopamine and 29% for quercetin). Superhydrophobic electrodes have achieved sensitive detection of dopamine and quercetin with LODs of 0.25 μM and 0.5 μm, respectively. Self-cleaning superhydrophobic electrodes can be combined with the magneto-controlled moveable architecture (MCMA) strategy for detecting carcinoembryonic antigen (CEA). This work achieved linear detection ranges of 0.1–100 ng mL^{-1} and a LOD of 0.041 ng mL^{-1}. Due to its self-cleaning properties,

© 2022 The Author(s). Published by the Royal Society of Chemistry

Open Access Article. Published on 23 marec 2022. Downloaded on 19. 06. 2025 12:07:07.
This article is licensed under a Creative Commons Attribution-NonCommercial 3.0 Unported Licence.

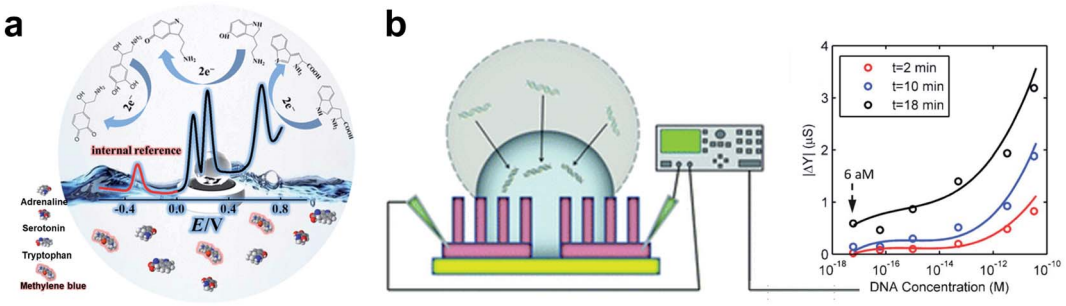

Fig. 5 Biosensors based on the superhydrophobic electrodes. (a) The combination of the self-cleaning superhydrophobic electrode with the ratiometric strategy for Adrenaline, Serotonin, and Tryptophan detection. Reproduced from ref. 106 with permission. Copyright 2019, American Chemical Society. (b) The droplet evaporation on the nanotextured superhydrophobic electrode for DNA enrichment. Adapted from ref. 108 with permission. Copyright 2013, Royal Society of Chemistry.

the superhydrophobic electrode can be used repetitively by simple washing for the desorption of the MCMA.

The self-cleaning superhydrophobic electrode was also combined with a ratiometric strategy for complex detection, as shown in Fig. 5a. Zhang *et al.* developed a self-cleaning electrode by modifying the zeolite imidazole framework (ZIF) and PDMS on the GCE.[106] The ratiometric strategy was built by introducing methylene blue as a reference molecule into the electrolyte solution, which avoids tedious modification of electrodes. The superhydrophobic electrode has proved to be stable in air for 45 days due to its great self-cleaning ability. And the reproducibility was verified by repeatedly polishing and remanufacturing with an average RSD of 6.67%. Moreover, the integrated biosensor has presented good sensitivity in multiple biomarker detection (LOD of 0.13 μM for Adrenaline, 0.03 μM for Serotonin, and 0.5 μM for Tryptophan). The superhydrophobicity of the fabricated electrodes is beneficial for refresh ability and stability of the electrode, improving the reproducibility of detection results.

Biomarker enrichment can effectively improve the detection sensitivity of low-abundance biomarkers.[107] Evaporation of sample droplets is an efficient method to achieve biomarker enrichment.[48] The droplet evaporation process on solid surfaces can be divided into two modes: constant contact area mode and constant contact angle mode. Droplet evaporation on surfaces with high contact angle hysteresis usually adopts constant contact area evaporation. In contrast, evaporation on the surface with low contact angle hysteresis is constant contact angle evaporation. Alam's group has developed a nanotextured superhydrophobic electrode array for ultratrace biomarker analysis, as shown in Fig. 5b.[108] The high roughness of the nanotextured surface provided superhydrophobicity with high contact angle hysteresis. Droplet evaporation on the fabricated superhydrophobic electrode followed the constant area mode, and the three-phase contact line did not move backward. Thus, the enrichment of biological samples and signal enhancement were achieved. In addition, the thermal effect of the electrodes in the detection process accelerates the evaporation process of the droplets. The superhydrophobic electrode has exhibited ultra-high sensitivity towards label-free DNA detection with a LOD of 60 aM by non-faradaic impedance spectroscopy. Superhydrophobic electrodes give insight into ultra-trace sample detection and will have broad application in biosensing.

Superaerophilic/superaerophobic electrodes for electrochemical biosensing

In some gas involving electrochemical reactions, the contact state between the gas and electrode interface will affect the thermodynamics of the reaction.[53,109] Gas involving electrochemical reactions can be divided into gas consumption reactions and gas evolution reactions.[59] For gas consumption reactions, increasing the gas concentration can promote the forward progress of the reaction.[110] In contrast, accelerating the desorption and escape of the gas is the key process to promote the progress of gas evolution reactions.[111,112]

Inspired by bubble bursting on the surface of lotus leaves, many superaerophilic surfaces have been fabricated.[113]Superaerophilic electrodes are electrodes with high gas affinity. The rough superaerophilic electrode can trap air bubbles on the surface when immersed into the electrolyte solution (Fig. 3b left), and a liquid–gas–solid triphase interface formed.[114] Since the diffusion coefficient of the gas in the liquid phase is much lower than that in the gas phase, the triphase interface on superaerophilic electrodes can provide a stable and abundant concentration of the gas reactant, which favors the forward process for those gas consumption reactions. The electrochemical glucose detection is a typical gas consumption reaction, where oxygen is the main reactant. The stable oxygen concentration at the electrode surface is critical for glucose biosensing.[115] The liquid–gas–solid triphase interface induced by the superaerophilic electrode will provide an abundance of oxygen. Feng's group has developed an oxygen-rich enzyme biosensor for glucose detection based on the superaerophilic electrode.[88] As shown in Fig. 6a (left), the superaerophilic electrode was fabricated by modifying a catalyst (*e.g.*, Pt) and oxidase (*e.g.*, glucose oxidase) on an underwater superaerophilic (*i.e.* superhydrophobic substrate) carbon fiber substrate. The superaerophilic electrode has been used for glucose detection and achieved a large linear detection range (up to156 mM), which is much higher than the linear detection range (up to 5 mM) of the GCE, as shown in Fig. 6a right. Furthermore, the

Open Access Article. Published on 23 marec 2022. Downloaded on 19. 06. 2025 12:07:07.
This article is licensed under a Creative Commons Attribution-NonCommercial 3.0 Unported Licence.

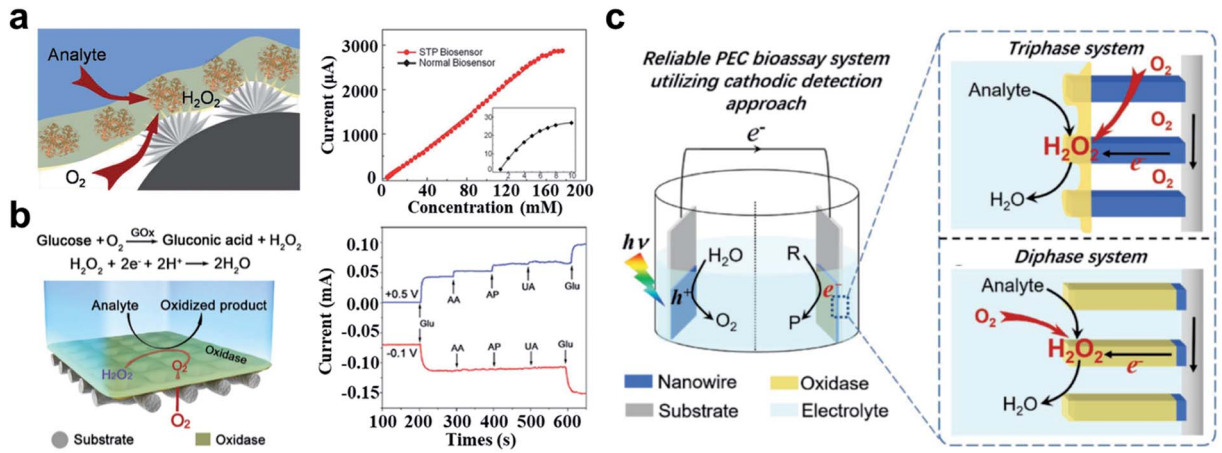

Fig. 6 Applications of the underwater superaerophilic electrode for glucose detection. (a) The triphase interface induced by the superaerophilic electrode for gas involving biosensing (left). Superaerophilic electrode (red line) shows a larger linear detection range than a flat electrode (black line) (right). Adapted from ref. 88 with permission. Copyright 2016, Wiley-VCH. (b) The H_2O_2 cathodic reaction for glucose detection based on the superaerophilic electrode (left). The cathodic reaction (red line) exhibits better interference resistance compared to the anodic reaction (blue line) (right). Adapted from ref. 116 with permission. Copyright 2018, Wiley-VCH. (c) The PEC bioassay system based on the superaerophilic electrode. Compared with the diphase system, the triphase system provided sufficient oxygen content. Adapted from ref. 117 with permission. Copyright 2018, Wiley-VCH.

superaerophilic electrode exhibited excellent stability by measuring 20 mM glucose 120 times with a relative standard deviation of 1.1%.

In the detection of glucose, there are many interferences (*e.g.*, ascorbic acid (AA), homovanillic acid (HVA), and uric acid (UA)) in the anodization reaction. In contrast, the H_2O_2 cathodic reduction reaction can avoid these interferences in glucose detection in complex solutions. Since the reduction potential of oxygen is similar to that of H_2O_2 reduction, the unstable oxygen concentration will result in inconsistent background signal. Due to the triphase interface, the oxygen concentration in the system is stable, resulting in a stable background signal. Song *et al.* developed a superaerophilic electrode for H_2O_2 cathodic detection as shown in Fig. 6b (left).[116] Compared with normal electrodes, superaerophilic electrodes showed stable signals in solutions with different oxygen contents. The cathodic reduction reaction has effectively avoided the interference of other substances (Fig. 6b right). The detection of glucose based on the superaerophilic electrode was achieved in a linear dynamic range of 80×10^{-3} M, which is significantly higher than that of a standard GCE (0.7×10^{-3} M). The superaerophilic electrode has provided a novel strategy by introducing a triphase reaction interface that caused sufficient gas supply for gas consumption biosensors. In addition, superaerophilic electrodes have also been used in photoelectrochemical (PEC) bioassays. Wang *et al.* developed a PEC bioassay system based on the cathode reaction as shown in Fig. 6c.[117] The superaerophilic electrode has provided a stable concentration of O_2 due to the triphase interface. Such superaerophilic electrode-based PEC biosensors have been applied in glucose detection and achieved high sensitivity with a LOD of 1×10^{-6} M. The linear detecting range of the triphase electrode is 100 times higher than that of the diphase one.

The triphase interface based on the superaerophilic electrode can be applied as a versatile platform for other gas consumption reactions and provides an optional way to fabricate highly sensitive biosensors with gas involved.

Electrochemical water splitting has been considered an efficient and sustainable strategy to produce clean fuels. In the hydrogen evolution reaction, hydrogen gas bubbles are produced, and generally adhere to the electrodes and desorb when grown to a critical size (about a few hundred μm). These bubbles hinder the contact between the electrolyte and the electrode and reduce the electrochemical catalytic efficiency.[118] The superaerophobic surface has low adhesion to gas bubbles (Fig. 3b right), and can facilitate the desorption and escape of gas bubbles on the electrode surface. This unique property will promote the forward progress of some gas evolution electrochemical reactions. Sun's group has developed an underwater superaerophobic electrode based on the MoS_2 nanostructured film for a highly efficient hydrogen evolution reaction (HER), as shown in Fig. 7a left.[92] The superaerophobic electrode has exhibited good HER efficiency (Fig. 7a right), which can be higher than the HER efficiency of commercial Pt/C films at sufficiently high overpotentials. On the superaerophobic electrode, the bubbles desorb and escape before reaching 100 μm in diameter. The superhydrophobic electrode exhibits anti-bubble adhesion performance compared with the flat electrode (bubbles diameter more than 400 μm). They also developed a superaerophobic electrode based on a pine-shaped Pt nanoarray for the HER as shown in Fig. 7b left.[119] The pine-shaped Pt nanoarray electrode exhibited a high electrochemically active surface area, which is twice that of the flat electrode. Compared with spherical nanostructured electrodes with similar electroactive surface areas, the pine-shaped Pt nanoarray electrodes exhibited better HER performance (2.55 times higher) due to better bubble repulsion induced by the unique nanostructures.

© 2022 The Author(s). Published by the Royal Society of Chemistry

Open Access Article. Published on 23 marec 2022. Downloaded on 19. 06. 2025 12:07:07.
This article is licensed under a Creative Commons Attribution-NonCommercial 3.0 Unported Licence.

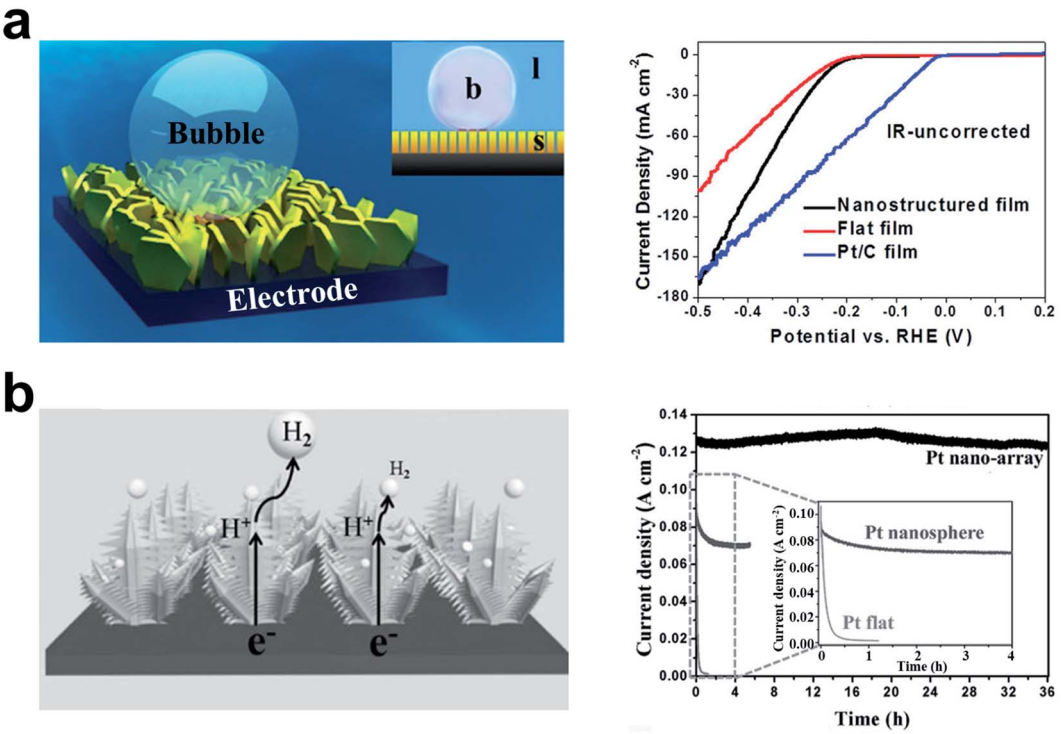

Fig. 7 The highly efficient HER on an underwater superaerophobic electrode. (a) Schematic of the adhesion behavior of bubbles on the superaerophobic electrode (left). The superaerophobic electrode (nanostructured film) showed high HER performance compared with flat films and Pt/C films, (right). Adapted from ref. 92 with permission. Copyright 2014, Wiley-VCH. (b) The pine-shaped Pt nanoarray superaerophobic electrode for the HER (left). Pine-shaped Pt nanoarray superaerophobic electrode showed good long-term stability compared with the Pt nanosphere electrode and the Pt flat electrode (right). Adapted from ref. 119 with permission. Copyright 2015, Wiley-VCH.

Furthermore, the pine-shaped Pt nanoarray electrode has showed steady HER performance (about 100% retention) over 36 hours of stability measurements (Fig. 7b right). This work revealed the relationship between electrode wettability and sensing performance and provided a new approach to developing highly efficient electrodes for gas evolution reactions.

Due to their extraordinary low adhesion to gas bubbles, nanostructured superaerophobic electrodes favor gas evolution reactions, which might be very promising in developing efficient electrochemical assays with gas products, such as H_2O_2 detection.

Superwettable micropatterned electrodes for electrochemical biosensors

Inspired by desert beetles, superwettable micropatterns have been fabricated by combining superhydrophobic backgrounds with superhydrophilic microwells.[120] Superwettable patterns have been broadly applied in biosensors due to their several advantages, including: (1) superhydrophilic microwells provide stable droplet anchoring ability; (2) the superhydrophobic background prevents contamination between adjacent droplets; (3) the evaporation of droplet enables ultratrace sample enrichment; (4) the small size of the superhydrophilic microwells allows low sample consumption; (5) the superhydrophilic microwell array allows multiplex detection.[47,55,121–123]

Our group has combined the superwettable micropattern microchip with the dual-DNA walker strategy to detect *E. coli* O157: H7 DNA.[124] The microchip was prepared based on a fractal gold substrate. The superhydrophobic background prevents the liquid from spreading, and the superhydrophilic microwells provide the point of liquid anchoring. Such a synergistic effect has provided good droplet management and significantly reduced the amount of the analytical solution. Moreover, the nanostructured fractal gold has provided a large contact area to enhance the response signal. The microchip has achieved ultrahigh sensitive detection of the *E. coli* O157: H7 DNA with a LOD of 30 aM. In addition, we also used the superwettable micropatterned microchip for the multiplex detection of prostate cancer biomarkers (miRNA-375, miRNA-141, and prostate-specific antigen), as shown in Fig. 8a.[125] The superhydrophobic background has successfully prevented the inter-contamination of adjacent droplets. And the multi-biomarker sensitive detection has proved that the LODs of miRNA-141 and miRNA-375 are 0.8 nM, and the PSA is 1.0 pM. The superwettable micropatterned electrodes have presented great potential in multiplex electrochemical analysis.

Levkin's group has developed a superwettable droplet array based on orthometric gold electrode bands (Fig. 8b).[126] The superwettable droplet array was fabricated by covering superwettable patterned porous polymethacrylate on orthometric gold electrode bands. Each superhydrophilic well can act as an individual electrochemical assay without the inter-contamination of adjacent droplets and ion transport. The individual droplet cell array was obtained by rolling liquid on the surface

Open Access Article. Published on 23 marec 2022. Downloaded on 19. 06. 2025 12:07:07.
This article is licensed under a Creative Commons Attribution-NonCommercial 3.0 Unported Licence.

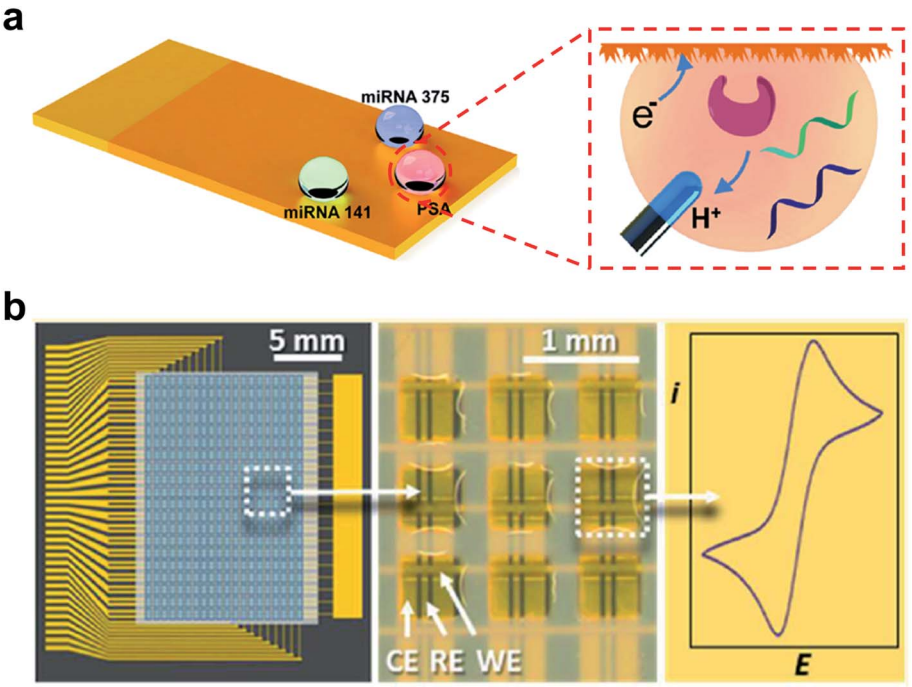

Fig. 8 The superwettable micropatterned electrode-based microchip for electrochemical analysis. (a) The miRNAs and PSA electrochemical analysis on the superwettable patterned microchip. Adapted from ref. 125 with permission. Copyright 2018, American Chemical Society. (b) The electrochemical analysis in the droplet microarray based on orthometric gold electrode bands. Reproduced from ref. 126 with permission. Copyright 2017, American Chemical Society.

of the electrode. The electrochemical signal of each droplet in the array can be read out individually. The sensitive detection ability of 1,4-benzoquinone and H_2O_2 within a single droplet has been confirmed.

Electrodes with switchable wettabilities

The coupling of the amplification-by-wettability switching concept with the electrochemical method offers great promise in bio-detection. The surface with switchable wettabilities in response to the external stimulus (pH value, irradiation, heat, or some molecules) was explored.[127] Adding some biomolecules (saccharides, nucleic, or protein) can induce hydrogen-boding interactions between the polymer substrate and biomolecules, which incurs wettability switching. The biomarker responded switchable surface could be applied for fabricating electrochemical biosensors.[49,128,129]

Ding *et al.* developed a wettability switchable electrode for chiral sensing of monosaccharide enantiomers.[56] As shown in Fig. 9, the presence of monosaccharide induces enantiomer conformational transition of the copolymer, which further results in the transformation of wettability and facilitates the diffusion of electroactive probes to the electrode. In the absence of target monosaccharides, the copolymer consisting of poly(*N*-isopropylacrylamide) (PNI), β-Asp-Phe dipeptide (β-MAP), and bis(trifluoromethyl)-modified phenylthiourea (TP) can form intramolecular hydrogen bonds, which results in the contraction of the copolymer chains and superhydrophobic surface. When different chiral monosaccharide enantiomers were present, the intramolecular hydrogen bonds of the copolymer were broken to different extents, which further resulted in the switching of the wettability from hydrophobicity to hydrophilicity. The change of electrode wettability favors the enrichment of the target on the screen-printed carbon electrode (SPCE) and further improves the sensitivity of electrochemical detection. Such a wettability switchable electrode has achieved sensitive detection of D-glucose as observed by electrochemical impedance spectroscopy with a LOD of 1 nM. In addition, electrodes with switchable wettabilities have been employed to monitor the D-glucose uptake behavior of cancer cells.

According to the same strategy, an electrode with switchable wettability in response to sialic acid (SA) has been fabricated for SA electrochemical biosensing.[130] The modified SPCE/Au electrode can switch from superhydrophobic to superhydrophilic

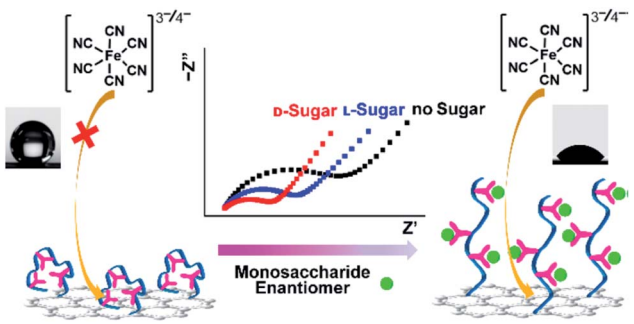

Fig. 9 Schematic of wettability switchable electrodes for chiral sensing of monosaccharide enantiomers. Reproduced from ref. 56 with permission. Copyright 2016, American Chemical Society.

© 2022 The Author(s). Published by the Royal Society of Chemistry

Open Access Article. Published on 23 marec 2022. Downloaded on 19. 06. 2025 12:07:07.
This article is licensed under a Creative Commons Attribution-NonCommercial 3.0 Unported Licence.

with the presence of SA, which further allows the enrichment of redox labels and targets on the electrode surface, thus enhancing the electrochemical signal response. Sensitive SA detection (LOD 0.4 pM) was achieved based on the electrode with switchable wettability. The dynamic monitoring of SA in a living mouse brain was also performed by combining with *in vivo* microdialysis.

Electrodes with switchable wettability have shown excellent selectivity due to their inherent specificity molecule recognition system. Such electrodes have indicated broad applications in highly specific biomarker monitoring in complex samples.

Superwettable materials for wearable electrochemical sensors

Wearable electrochemical sensors have garnered considerable attention due to their tremendous promise in real-time and non-invasive monitoring of chemical markers and physical signals.[131–133] Through the modality of accessories or clothes, sweat components (including glucose, sodium and potassium ions, and pH) can be non-invasively detected by the wearable electrochemical sensor.[134–137] Connecting wearable electrochemical sensors to mobile devices (*e.g.*, mobile phones and tablet computers) can achieve real-time, user-friendly, and household/bedsides monitoring.[138] Superwettable materials have been used in wearable biosensors and provide unique sample management capabilities.[139]

Eccrine sweat is a significant biofluid containing rich biomarkers ranging from electrolytes, metabolites, hormones to proteins. Sweat collection is critical for wearable biosensors.[138] Current sweat collection relies on absorbent pads adhering to the skin. He *et al.* recently developed a wearable sweat sensor based on a superhydrophilic carbon textile derived from silk fabrics for six sweat biomarker simultaneous detection (Fig. 10a).[140] A superhydrophilic nitrogen-doped carbon textile (SilkNCT) was integrated on a flexible PET substrate as the working electrode. The hydrophobic PET substrate can separate the six working electrodes and avoid inter-contamination. The superhydrophilic SilkNCT has provided excellent sweat collection ability and shown good sensitivity for detecting glucose, lactate, ascorbic acid, uric acid, Na^+ and K^+, and the LODs are 5 μM, 0.5 mM, 0.5 mM, 0.1 μM, 1 mM and 0.5 mM, respectively. The excellent reproducibility was confirmed with relative standard deviations (RSD) for six biomarkers ≤ 8.2%. In addition, the SilkCNT-based wearable biosensor combined with mobile phones enabled real-time monitoring of the glucose concentration.

As has been discussed previously, the triphase interface can provide a stable and abundant concentration of gas reactants. Lei *et.al.* combined the MXene-based superhydrophobic electrode with wearable biosensors for the detection of glucose and lactate in sweat as shown in Fig. 10b.[141] The MXene-based superhydrophobic electrode exhibited high gas affinity and

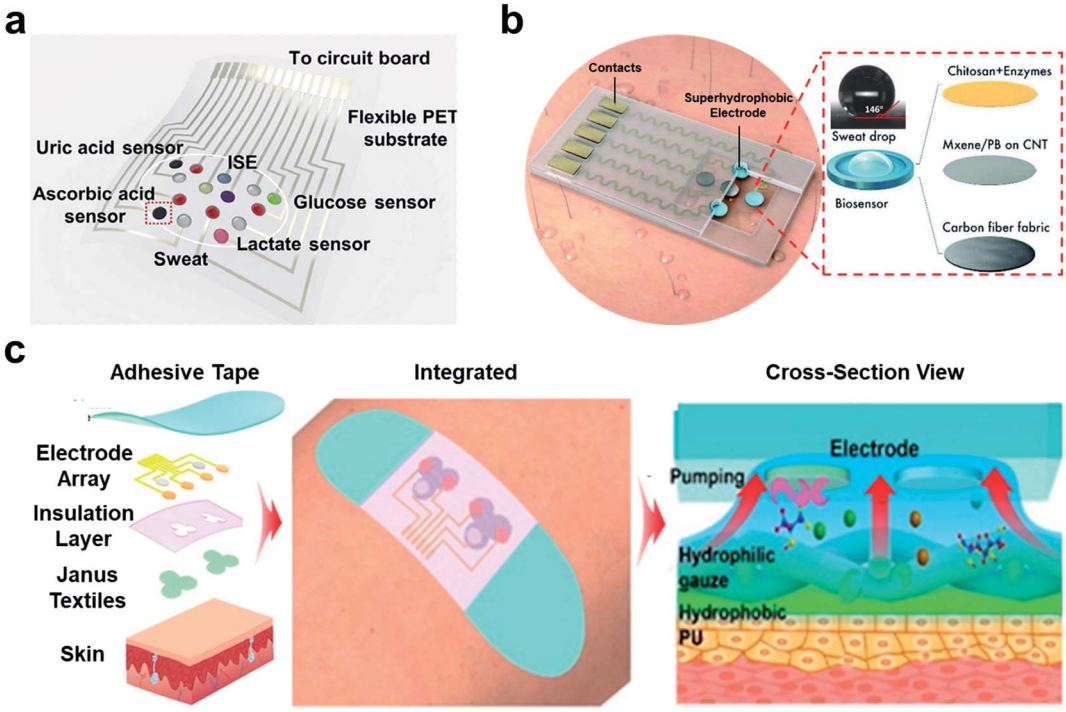

Fig. 10 Superwettable materials in wearable electrochemical biosensors. (a) The wearable biosensor based on the superhydrophilic electrodes for the multiplex sweat analysis. Adapted from ref. 140 with permission. Copyright 2019, AAAS. (b) The superhydrophobic (superaerophilic) electrode integrated wearable biosensor for gas-involving on-body analysis. Adapted from ref. 141 with permission. Copyright 2019, Wiley-VCH. (c) Wearable sweat sensor based on the Janus electrode for sweat transportation and analysis. The Janus electrode transported the sweat from the hydrophobic side to hydrophilic side for sample enrichment. Adapted from ref. 148 with permission. Copyright 2020, American Chemical Society.

© 2022 The Author(s). Published by the Royal Society of Chemistry

Open Access Article. Published on 23 marec 2022. Downloaded on 19. 06. 2025 12:07:07.
This article is licensed under a Creative Commons Attribution-NonCommercial 3.0 Unported Licence.

Table 1 The properties of superwettable electrodes in electrochemical biosensing

Type	Interfacial property	Sensing Performance	Limitation
Superhydrophilic electrode	Large electroactive area	Signal enhancement	High sample consumption for bulk electrodes
		Accelerating recognition dynamics	Nonspecific adsorption
			Reproducibility needs to be improved
			Expensive
Superhydrophobic electrode	Self-cleaning	Good reproducibility	Unstable superhydrophobicity
	Small contact area	Sample enrichment	Difficulty in anchoring droplets
Superaerophilic electrode	High gas affinity	Enrichment of gas reactant	Only for gas consumption reactions
		Promoting gas consumption reactions	
Superaerophobic electrode	Gas repelling	Accelerating gas product desorption	Only for gas evolution reactions
		Promoting gas evolution reactions	
Superwettable patterned electrode	Patterned hydrophilicity and hydrophobicity	Liquid manipulation	Reproducibility needs to be improved
		Sample enrichment	Nonspecific adsorption in hydrophilic zone
		Low sample consumption	
		High-throughput	
Wettability switchable electrode	Stimuli response wettability change	High selectivity	Not versatile
Janus wettability electrode	Asymmetric wettability	Sample directional transport	Reproducibility needs to be improved
			Nonspecific adsorption in hydrophilic side

formed a stable liquid–gas–solid triphase interface. The existence of the triphase interface promised a high abundant concentration of oxygen during the detection process. The superaerophilic electrode presented high electrochemical sensitivity in the detection of glucose (35.3 μA mm^{-1} cm^{-2}) and lactate (11.4 μA mm^{-1} cm^{-2}) with LODs of 0.33×10^{-6} M and 0.67×10^{-6} M respectively. And the glucose values during the on-body tests showed good agreement with the reported blood and sweat glucose levels very well.

Inspired by the binary synergistic wettability of lotus leaves, Janus films with asymmetric wettability have been developed and are promising in various fields, including water harvesting, fog collection, liquid separation, microfluidics, and wound dressing.[142–146] Incorporating Janus films with wearable biosensors can achieve the directional transport of sweat. The hydrophobic side of Janus films was placed on the skin. When sweat was secreted, the capillary force helped sweat transport from the hydrophobic side to the superhydrophilic side.[147] The collected sweat was retained in the superhydrophilic side for sample enrichment. Compared to the ordinary gauze, the Janus band showed excellent sweat transportation, resulting in an almost dry skin side. He *et al.* presented a Janus wettability textile strategy to transport sweat from the skin to the embedded electrode surface for the directional collection of sweat (Fig. 10c).[148] A Janus band was developed by combining a hydrophobic polyurethane (PU) and a superhydrophilic gauze through the electrospinning process. The PU side was covered on the skin, and the superhydrophilic side was linked to the electrode. The Janus band has shown good sensitivity in glucose (8 nA μM^{-1}), lactate (67 nA μM^{-1}), Na^+ (35.0 mV dec^{-1}), and K^+ (45.6 mV dec^{-1}). The on-body test can achieve real-time perspiration tracking, and the results were in good agreement with the physiological indicators of healthy people. In addition, Janus materials with sweat management can conduct thermal management on wearable biosensors. They have developed a Janus silk-based wearable sweat electrochemical biosensor with good wet-thermal comfort.[57] A conductive silk yarn electrode was woven into the Janus silk. When sweat was transported, the signal can be directly recorded, processed, and transmitted by the connected printed circuit board. The directional transport of the sweat ensures good thermal and humidity management, which improves the wearing comfort. The silk electrode showed excellent electrochemical stability through 800 cycle bending and a sensitive response to glucose (0.49 nA μM^{-1}), urine acid (1.703 nA μM^{-1}), pH (62.25 mV/$lg(H^+)$) and K^+ (67.44 mV/$lg(K^+)$). And the Janus silk showed a higher response rate than the ordinary silk in the on-body measurements due to its good ability of sweat transportation.

Conclusion and outlook

In this review, recent developments in bioinspired electrodes with special wettability have been summarized. The special structure and interfacial properties of superwettable electrodes have injected new vitalities to electrochemical biosensing, which are listed in Table 1. Research on electrodes with special wettabilities not only has fundamental interest but also promising practical applications in biomarker detection, clinical diagnosis, environment monitoring, food safety, and so on. Superwettable electrodes have exuded unique advantages in promoting the electrochemical reaction such as accelerating component transport, enhancing sensitivity and selectivity, and

© 2022 The Author(s). Published by the Royal Society of Chemistry

Open Access Article. Published on 23 marec 2022. Downloaded on 19. 06. 2025 12:07:07.
This article is licensed under a Creative Commons Attribution-NonCommercial 3.0 Unported Licence.

target solution management. However, most superwettable electrodes are limited to laboratory research and have not yet been applied to practical applications and industrial-scale production. Thus there are some challenges including the cost of biosensor construction and the long-term storage ability of the electrode to be addressed.

1. Cost is the most crucial parameter in industrial manufacture and diagnostic application. Most superwettable electrodes are based on expensive noble metals. Nanostructured conductive polymer materials might be a good alternative in fabricating electrodes with special wettability. Moreover, the fabrication process for superwettable electrodes is limited to laboratory research and not suitable for industrial scale. Therefore, there is an urgent need for a stable and efficient engineering method to lower the fabrication cost.

2. The mechanical stability and durability of superwettable electrodes are significant in practical applications. The collapse of the surface structure may result in instability of wettability. In this case, self-healing and self-replenishing materials (such as hydrogel or slippery surfaces) may be helpful in fabricating superwettable electrodes with long-term stability under different physical conditions.

3. For now, the surface structures of many organisms have been revealed. Bioinspired materials with special wettability (Fig. 3) based on these special surfaces have also been developed and widely used in many ways. However, these surfaces have not been explored for electrochemical sensors. Extending the concept of superwettable electrodes to water/oil/solid systems might be crucial for bio-detection in complex samples.

4. The understanding of wetting and adhesion of reactants/products at superwettable electrodes at the molecular level remains obscure. More effort should be contributed to theoretical calculations and simulations to enhance the fundamental understanding. The relationship between the surface wettability of superwettable electrodes and the biosensor performances should be intensively studied.

Although the study about superwettable electrodes in biosensing is still in its infancy, numerous opportunities are emerging ranging from chemistry and materials science to clinical applications. With the rapid development of biomimetic superwettable materials, a variety of surfaces with special wettability have been successfully fabricated. In the future, more electrodes with special wettable interfaces will be developed to meet the requirements of various electrochemical biosensors. Given the continuous efforts devoted to this field, we are confident that superwettable surfaces may not only possess tremendous potential in biosensing but also provide many insights for other multiphase reaction systems.

Author contributions

Li-Ping Xu and Shutao Wang conceptualized the paper. Qinglin Zhu, Yuemeng Yang and Hongxiao Gao prepared the original draft of the manuscript. Qinglin Zhu, Li-Ping Xu and Shutao Wang reviewed and edited its contents. Li-Ping Xu and Shutao Wang supervised the work.

Conflicts of interest

The authors declare no conflicts.

Acknowledgements

This work was financially supported by the National Key R&D Program of China (2019YFA0709300), National Natural Science Foundation of China (21890742, 22035008, 21972155 and 21988102), Beijing Municipal Science and Technology Commission (2182036), and International Partnership Program of Chinese Academy of Sciences (1A1111KYSB20200010).

References

1 L. Feng, S. Li, Y. Li, H. Li, L. Zhang, J. Zhai, Y. Song, B. Liu, L. Jiang and D. Zhu, *Adv. Mater.*, 2002, **14**, 1857.
2 K. Koch and W. Barthlott, *Philos. Trans. R. Soc., A*, 2009, **367**, 1487.
3 M. Liu, S. Wang, Z. Wei, Y. Song and L. Jiang, *Adv. Mater.*, 2009, **21**, 665.
4 H. Chen, P. Zhang, L. Zhang, H. Liu, Y. Jiang, D. Zhang, Z. Han and L. Jiang, *Nature*, 2016, **532**, 85.
5 K. Liu and L. Jiang, *ACS Nano*, 2011, **5**, 6786.
6 P. Zhang, S. Wang, S. Wang and L. Jiang, *Small*, 2015, **11**, 1939.
7 B. Su, L. Jiang, X. Jiang and A. Yu, *Powder Technol.*, 2017, **312**, 103.
8 Q. Wen, J. Di, Y. Zhao, Y. Wang, L. Jiang and J. Yu, *Chem. Sci.*, 2013, **4**, 4378.
9 F. Gomollón-Bel, *Chem. Int.*, 2021, **43**, 13.
10 R. Blossey, *Nat. Mater.*, 2003, **2**, 301.
11 Y. Zheng, H. Bai, Z. Huang, X. Tian, F. Q. Nie, Y. Zhao, J. Zhai and L. Jiang, *Nature*, 2010, **463**, 640.
12 M. J. Kreder, J. Alvarenga, P. Kim and J. Aizenberg, *Nat. Rev. Mater.*, 2016, **1**, 15003.
13 E. Hermelin, J. Petitjean, J.-C. Lacroix, K. I. Chane-Ching, J. Tanguy and P.-C. Lacaze, *Chem. Mater.*, 2008, **20**, 4447.
14 Z. Xue, S. Wang, L. Lin, L. Chen, M. Liu, L. Feng and L. Jiang, *Adv. Mater.*, 2011, **23**, 4270.
15 A. Tricoli, M. Righettoni and S. E. Pratsinis, *Langmuir*, 2009, **25**, 12578.
16 D. Tian, Y. Song and L. Jiang, *Chem. Soc. Rev.*, 2013, **42**, 5184.
17 Y. Chen, X. Min, X. Zhang, F. Zhang, S. Lu, L. P. Xu, X. Lou, F. Xia, X. Zhang and S. Wang, *Biosens. Bioelectron.*, 2018, **111**, 124.
18 T. Wu, T. Xu, L. P. Xu, Y. Huang, W. Shi, Y. Wen and X. Zhang, *Biosens. Bioelectron.*, 2016, **86**, 951.
19 F. Narita, Z. Wang, H. Kurita, Z. Li, Y. Shi, Y. Jia and C. Soutis, *Adv. Mater.*, 2021, **33**, 2005448.
20 H. Zhu, Y. Huang, X. Lou and F. Xia, *View*, 2020, **2**, 20200053.
21 S. Zhan, Y. Pan, Z. F. Gao, X. Lou and F. Xia, *Trends Anal. Chem.*, 2018, **108**, 183.
22 J. Ping, Z. Fan, M. Sindoro, Y. Ying and H. Zhang, *Adv. Funct. Mater.*, 2017, **27**, 1605817.

Open Access Article. Published on 23 marec 2022. Downloaded on 19. 06. 2025 12:07:07.
This article is licensed under a Creative Commons Attribution-NonCommercial 3.0 Unported Licence.

23 Y. Chen, L. P. Xu, J. Meng, S. Deng, L. Ma, S. Zhang, X. Zhang and S. Wang, *Biosens. Bioelectron.*, 2018, **102**, 418.
24 T. Wu, T. Xu, Y. Chen, Y. Yang, L.-P. Xu, X. Zhang and S. Wang, *Sens. Actuators, B*, 2018, **258**, 715.
25 T. Wu, Y. Yang, Y. Cao, Y. Song, L. P. Xu, X. Zhang and S. Wang, *ACS Appl. Mater. Interfaces*, 2018, **10**, 42050.
26 Z. F. Gao, R. Liu, J. Wang, J. Dai, W.-H. Huang, M. Liu, S. Wang, F. Xia and L. Jiang, *Chem*, 2018, **4**, 2929.
27 J. Das, I. Ivanov, L. Montermini, J. Rak, E. H. Sargent and S. O. Kelley, *Nat. Chem.*, 2015, **7**, 569.
28 Y. Song, T. Xu, L. P. Xu and X. Zhang, *Chem. Commun.*, 2019, **55**, 1742.
29 T. Xu, W. Shi, J. Huang, Y. Song, F. Zhang, L. P. Xu, X. Zhang and S. Wang, *ACS Nano*, 2017, **11**, 621.
30 Y. Song, T. Xu, L. P. Xu and X. Zhang, *Nanoscale*, 2018, **10**, 20990.
31 Y. Chen, K. Li, S. Zhang, L. Qin, S. Deng, L. Ge, L. P. Xu, L. Ma, S. Wang and X. Zhang, *ACS Nano*, 2020, **14**, 4654.
32 Y. Li, Y. Cheng, L. Xu, H. Du, P. Zhang, Y. Wen and X. Zhang, *Nanomaterials*, 2016, **6**, 24.
33 X. He, T. Xu, W. Gao, L. P. Xu, T. Pan and X. Zhang, *Anal. Chem.*, 2018, **90**, 14105.
34 Q. Zhu, T. Xu, Y. Song, Y. Luo, L. Xu and X. Zhang, *Biosens. Bioelectron.*, 2020, **158**, 112185.
35 T. Xu, Y. Luo, C. Liu, X. Zhang and S. Wang, *Anal. Chem.*, 2020, **92**, 7816.
36 H. Chen, Y. Fan, N. Zhang, S. Trepout, B. Ptissam, A. Brulet, B. Z. Tang and M. H. Li, *Chem. Sci.*, 2021, **12**, 5495.
37 L. Wu and X. Qu, *Chem. Soc. Rev.*, 2015, **44**, 2963.
38 A. Suea-Ngam, P. D. Howes and A. J. deMello, *Chem. Sci.*, 2021, **12**, 12733.
39 D. Chen, Y. Wu, S. Hoque, R. D. Tilley and J. J. Gooding, *Chem. Sci.*, 2021, **12**, 5196.
40 W. Wen, X. Yan, C. Zhu, D. Du and Y. Lin, *Anal. Chem.*, 2017, **89**, 138.
41 Y. Xia, Y. Sun, H. Li, S. Chen, T. Zhu, G. Wang, B. Man, J. Pan and C. Yang, *Talanta*, 2021, **223**, 121766.
42 Y. Yang, Y. Zhao, F. Sun, T. You, Y. Gao and P. Yin, *Microchem. J.*, 2020, **159**, 105427.
43 J. Li, X. Gao, Z. Li, J. H. Wang, L. Zhu, C. Yin, Y. Wang, X. B. Li, Z. Liu, J. Zhang, C. H. Tung and L. Z. Wu, *Adv. Funct. Mater.*, 2019, **29**, 1808079.
44 M. Li, J. Wei, L. Ren, Y. Zhao, Z. Shang, D. Zhou, W. Liu, L. Luo and X. Sun, *Cell Rep. Phys. Sci.*, 2021, **2**, 100374.
45 C. Li, X. Hu, J. Lu, X. Mao, Y. Xiang, Y. Shu and G. Li, *Chem. Sci.*, 2018, **9**, 979.
46 M. Zhang, T. Zhao, C. Yu, Q. Liu, G. Wang, H. Yang, M. Yang, L. Jiang and M. Liu, *Nano Res.*, 2022, **15**, 557.
47 T. Xu, L. P. Xu, X. Zhang and S. Wang, *Chem. Soc. Rev.*, 2019, **48**, 3153.
48 W. Yulu, L. Fei, Y. Yang and L.-P. Xu, *Mater. Chem. Front.*, 2021, **5**, 5639.
49 J. Y. Shiu and P. L. Chen, *Adv. Funct. Mater.*, 2007, **17**, 2680.
50 L. Chen, X. Sheng, D. Wang, J. Liu, R. Sun, L. Jiang and X. Feng, *Adv. Funct. Mater.*, 2018, **28**, 1801483.
51 X. Zhu, Y. Chen, C. Feng, W. Wang, B. Bo, R. Ren and G. Li, *Anal. Chem.*, 2017, **89**, 4131.
52 L. P. Xu, S. Wang, H. Dong, G. Liu, Y. Wen, S. Wang and X. Zhang, *Nanoscale*, 2012, **4**, 3786.
53 L. Chen and X. Feng, *Chem. Sci.*, 2020, **11**, 3124.
54 H. Li, S. Chen, Y. Zhang, Q. Zhang, X. Jia, Q. Zhang, L. Gu, X. Sun, L. Song and X. Wang, *Nat. Commun.*, 2018, **9**, 2452.
55 M. Liu, L. Feng, X. Zhang, Y. Hua, Y. Wan, C. Fan, X. Lv and H. Wang, *ACS Appl. Mater. Interfaces*, 2018, **10**, 32038.
56 S. Ding, S. Cao, A. Zhu and G. Shi, *Anal. Chem.*, 2016, **88**, 12219.
57 X. He, C. Fan, T. Xu and X. Zhang, *Nano Lett.*, 2021, **21**, 8880.
58 Y. Yang, L. P. Xu, X. Zhang and S. Wang, *J. Mater. Chem. B*, 2020, **8**, 8101.
59 W. Xu, Z. Lu, X. Sun, L. Jiang and X. Duan, *Acc. Chem. Res.*, 2018, **51**, 1590.
60 M. Labib, E. H. Sargent and S. O. Kelley, *Chem. Rev.*, 2016, **116**, 9001.
61 M. Khademi and D. P. J. Barz, *Langmuir*, 2020, **36**, 4250.
62 R. Parsons, *Chem. Rev.*, 1990, **90**, 813.
63 G. Trefalt, S. H. Behrens and M. Borkovec, *Langmuir*, 2016, **32**, 380.
64 J. J. Bikerman, *Philos. Mag.*, 1942, **33**, 384.
65 S. Maheshwari, Y. Li, N. Agrawal and M. J. Janik, *Adv. Catal.*, 2018, **63**, 117.
66 Z. Erdelyi, *Scr. Mater.*, 2003, **49**, 613.
67 D. Andreucci, E. N. M. Cirillo, M. Colangeli and D. Gabrielli, *J. Stat. Phys.*, 2018, **174**, 469.
68 A. De Masi, I. Merola and E. Presutti, *J. Math. Phys.*, 2021, **62**, 073301.
69 M. Faraday, *Philos. Trans. R. Soc.*, 1834, **124**, 77.
70 F. W. Sears, *Am. J. phys.*, 1963, **31**, 439.
71 F. C. Strong, *J. Chem. Educ.*, 1961, **38**, 98.
72 W. B. Jensen, *J. Chem. Educ.*, 2012, **89**, 1208–1209.
73 S. Wang, L. P. Xu, H. W. Liang, S. H. Yu, Y. Wen, S. Wang and X. Zhang, *Nanoscale*, 2015, **7**, 11460.
74 Y. Jin, T. Qi, Y. Ge, J. Chen, L. Liang, J. Ju and J. Zhao, *Anal. Methods*, 2021, **13**, 996.
75 S. Wang, K. Liu, X. Yao and L. Jiang, *Chem. Rev.*, 2015, **115**, 8230.
76 Z. Ashrafi, L. Lucia and W. Krause, *ACS Appl. Mater. Interfaces*, 2019, **11**, 21275.
77 M. Liu, S. Wang and L. Jiang, *Nat. Rev. Mater.*, 2017, **2**, 17036.
78 Y. Tian and L. Jiang, *Nat. Mater.*, 2013, **12**, 291.
79 J. Drelich, E. Chibowski, D. D. Meng and K. Terpilowski, *Soft Matter*, 2011, **7**, 9804.
80 S. Wang and L. Jiang, *Adv. Mater.*, 2007, **19**, 3423.
81 R. N. Wenzel, *Ind. Eng. Chem.*, 1936, **28**, 988.
82 A. B. D. Cassie and S. Baxter, *Trans. Faraday Soc.*, 1944, **40**, 546.
83 C. A. Hamlett, N. J. Shirtcliffe, F. B. Pyatt, M. I. Newton, G. McHale and K. Koch, *Planta*, 2011, **234**, 1267.
84 F. Xia and L. Jiang, *Adv. Mater.*, 2008, **20**, 2842.
85 T. Sun, G. Wang, L. Feng, B. Liu, Y. Ma, L. Jiang and D. Zhu, *Angew. Chem., Int. Ed.*, 2004, **43**, 357.
86 T. Sun, G. Qing, B. Su and L. Jiang, *Chem. Soc. Rev.*, 2011, **40**, 2909.

© 2022 The Author(s). Published by the Royal Society of Chemistry

Open Access Article. Published on 23 marec 2022. Downloaded on 19. 06. 2025 12:07:07.
This article is licensed under a Creative Commons Attribution-NonCommercial 3.0 Unported Licence.

87 Z. Lu, W. Xu, J. Ma, Y. Li, X. Sun and L. Jiang, *Adv. Mater.*, 2016, **28**, 7155.
88 Y. Lei, R. Sun, X. Zhang, X. Feng and L. Jiang, *Adv. Mater.*, 2016, **28**, 1477.
89 M. J. Lee, H. P. Hong, K. H. Kwon, C. W. Park and N. K. Min, *Sens. Actuators, B*, 2013, **185**, 97.
90 S. Hu, Z. Shi, R. Zheng, W. Ye, X. Gao, W. Zhao and G. Yang, *ACS Appl. Mater. Interfaces*, 2020, **12**, 40021.
91 K. Liu and L. Jiang, *Nano Today*, 2011, **6**, 155.
92 Z. Lu, W. Zhu, X. Yu, H. Zhang, Y. Li, X. Sun, X. Wang, H. Wang, J. Wang, J. Luo, X. Lei and L. Jiang, *Adv. Mater.*, 2014, **26**, 2683.
93 C. Zhao, C. Ding, M. Lv, Y. Wang, L. Jiang and H. Liu, *RSC Adv.*, 2016, **6**, 22488.
94 Y. Peng, Y. Ning, X. Ma, Y. Zhu, S. Yang, B. Su, K. Liu and L. Jiang, *Adv. Funct. Mater.*, 2018, **28**, 1800712.
95 Y. Wu, J. Feng, H. Gao, X. Feng and L. Jiang, *Adv. Mater.*, 2019, **31**, 1800718.
96 J. Lyu, G. Sun, L. Zhu, H. Ma, C. Ma, X. Dong and Y. Fu, *J. Solid State Electrochem.*, 2019, **24**, 375.
97 Y. Liu, L. P. Xu, S. Wang, W. Yang, Y. Wen and X. Zhang, *Biosens. Bioelectron.*, 2015, **71**, 396.
98 B. Lam, Z. Fang, E. H. Sargent and S. O. Kelley, *Anal. Chem.*, 2012, **84**, 21.
99 L. Soleymani, Z. Fang, X. Sun, H. Yang, B. J. Taft, E. H. Sargent and S. O. Kelley, *Angew. Chem., Int. Ed.*, 2009, **48**, 8457.
100 X. Bin, E. H. Sargent and S. O. Kelley, *Anal. Chem.*, 2010, **82**, 5928.
101 H. Yang, A. Hui, G. Pampalakis, L. Soleymani, F. F. Liu, E. H. Sargent and S. O. Kelley, *Angew. Chem., Int. Ed.*, 2009, **48**, 8461.
102 P. Sadat Mousavi, S. J. Smith, J. B. Chen, M. Karlikow, A. Tinafar, C. Robinson, W. Liu, D. Ma, A. A. Green, S. O. Kelley and K. Pardee, *Nat. Chem.*, 2020, **12**, 48.
103 J. Das, K. B. Cederquist, A. A. Zaragoza, P. E. Lee, E. H. Sargent and S. O. Kelley, *Nat. Chem.*, 2012, **4**, 642–648.
104 D. G. Rackus, M. D. Dryden, J. Lamanna, A. Zaragoza, B. Lam, S. O. Kelley and A. R. Wheeler, *Lab Chip*, 2015, **15**, 3776.
105 K. Liu, X. Yao and L. Jiang, *Chem. Soc. Rev.*, 2010, **39**, 3240.
106 J. Zhang, D. Wang and Y. Li, *ACS Appl. Mater. Interfaces*, 2019, **11**, 13557.
107 I. Yanagimachi, N. Nashida, K. Iwasa and H. Suzuki, *Sci. Technol. Adv. Mater.*, 2005, **6**, 671.
108 A. Ebrahimi, P. Dak, E. Salm, S. Dash, S. V. Garimella, R. Bashir and M. A. Alam, *Lab Chip*, 2013, **13**, 4248.
109 D. Wang, Z. Ding, H. Zhou, L. Chen and X. Feng, *ACS Appl. Nano Mater.*, 2021, **4**, 9401.
110 L. Mi, J. Yu, F. He, L. Jiang, Y. Wu, L. Yang, X. Han, Y. Li, A. Liu, W. Wei, Y. Zhang, Y. Tian, S. Liu and L. Jiang, *J. Am. Chem. Soc.*, 2017, **139**, 10441.
111 S. Sheng, B. Shi, C. Wang, L. Luo, X. Lin, P. Li, F. Chen, Z. Shang, H. Meng, Y. Kuang, W. F. Lin and X. Sun, *ACS Appl. Mater. Interfaces*, 2020, **12**, 23627.
112 J. Yong, F. Chen, Y. Fang, J. Huo, Q. Yang, J. Zhang, H. Bian and X. Hou, *ACS Appl. Mater. Interfaces*, 2017, **9**, 39863.
113 J. Wang, Y. Zheng, F. Q. Nie, J. Zhai and L. Jiang, *Langmuir*, 2009, **25**, 14129.
114 F. Guan, J. Zhang, H. Tang, L. Chen and X. Feng, *Nanoscale Horiz.*, 2019, **4**, 231.
115 Q. Cheng, J. Zhang, H. Wang, D. Wang, X. Feng and L. Jiang, *Adv. Mater. Interfaces*, 2020, **7**, 1902172.
116 Z. Song, C. Xu, X. Sheng, X. Feng and L. Jiang, *Adv. Mater.*, 2018, **30**, 1701473.
117 D. Wang, L. Chen, J. Liu, F. Guan, R. Sun, L. Jiang and X. Feng, *Adv. Funct. Mater.*, 2018, **28**, 1804410.
118 C. Yu, P. Zhang, J. Wang and L. Jiang, *Adv. Mater.*, 2017, **29**, 1703053.
119 Y. Li, H. Zhang, T. Xu, Z. Lu, X. Wu, P. Wan, X. Sun and L. Jiang, *Adv. Funct. Mater.*, 2015, **25**, 1737.
120 A. R. Parker and C. R. Lawrence, *Nature*, 2001, **414**, 33.
121 C.-H. Kim, J.-H. Ahn, J.-Y. Kim, J.-M. Choi, T. J. Park and Y.-K. Choi, *Bionanoscience*, 2013, **3**, 192.
122 J. Y. Kim, K. Choi, D. I. Moon, J. H. Ahn, T. J. Park, S. Y. Lee and Y. K. Choi, *Biosens. Bioelectron.*, 2013, **41**, 867.
123 L. P. Xu, Y. Chen, G. Yang, W. Shi, B. Dai, G. Li, Y. Cao, Y. Wen, X. Zhang and S. Wang, *Adv. Mater.*, 2015, **27**, 6878.
124 X. Zhang, T. Wu, Y. Yang, Y. Wen, S. Wang and L.-P. Xu, *Sens. Actuators, B*, 2020, **321**, 128472.
125 T. Xu, Y. Song, W. Gao, T. Wu, L. P. Xu, X. Zhang and S. Wang, *ACS Sens.*, 2018, **3**, 72.
126 H. Zhang, T. Oellers, W. Feng, T. Abdulazim, E. N. Saw, A. Ludwig, P. A. Levkin and N. Plumere, *Anal. Chem.*, 2017, **89**, 5832.
127 G. Qing, X. Wang, L. Jiang, H. Fuchs and T. Sun, *Soft Matter*, 2009, **5**, 2759.
128 G. Qing, X. Wang, H. Fuchs and T. Sun, *J. Am. Chem. Soc.*, 2009, **131**, 8370.
129 G. Qing and T. Sun, *Adv. Mater.*, 2011, **23**, 1615.
130 S. Ding, S. Cao, Y. Liu, Y. Lian, A. Zhu and G. Shi, *ACS Sens.*, 2017, **2**, 394.
131 L. Wang, T. Xu and X. Zhang, *Trends Anal. Chem.*, 2021, **134**, 116130.
132 L. Wang, T. Xu, C. Fan and X. Zhang, *iScience*, 2021, **24**, 102028.
133 X. He, T. Xu, Z. Gu, W. Gao, L. P. Xu, T. Pan and X. Zhang, *Anal. Chem.*, 2019, **91**, 4296.
134 G. Li, X. Mo, W. C. Law and K. C. Chan, *ACS Appl. Mater. Interfaces*, 2019, **11**, 238.
135 C. W. Bae, P. T. Toi, B. Y. Kim, W. I. Lee, H. B. Lee, A. Hanif, E. H. Lee and N. E. Lee, *ACS Appl. Mater. Interfaces*, 2019, **11**, 14567.
136 K.-P. Gao, G.-C. Shen, N. Zhao, C.-P. Jiang, B. Yang and J.-Q. Liu, *IEEE Sens. J.*, 2020, **20**, 10393.
137 M. Li, L. Wang, R. Liu, J. Li, Q. Zhang, G. Shi, Y. Li, C. Hou and H. Wang, *Biosens. Bioelectron.*, 2021, **174**, 112828.
138 J. R. Sempionatto, I. Jeerapan, S. Krishnan and J. Wang, *Anal. Chem.*, 2020, **92**, 378.
139 K. Zhang, J. Zhang, F. Wang and D. Kong, *ACS Sens.*, 2021, **6**, 2261.
140 W. He, C. Wang, H. Wang, M. Jian, W. Lu, X. Liang, X. Zhang, F. Yang and Y. Zhang, *Sci. Adv.*, 2019, **5**, eaax0649.

© 2022 The Author(s). Published by the Royal Society of Chemistry

Open Access Article. Published on 23 marec 2022. Downloaded on 19. 06. 2025 12:07:07.
This article is licensed under a Creative Commons Attribution-NonCommercial 3.0 Unported Licence.

141 Y. Lei, W. Zhao, Y. Zhang, Q. Jiang, J. H. He, A. J. Baeumner, O. S. Wolfbeis, Z. L. Wang, K. N. Salama and H. N. Alshareef, *Small*, 2019, **15**, 1901190.
142 C. Zhang, Y. Zhang, X. Xiao, G. Liu, Z. Xu, B. Wang, C. Yu, R. H. A. Ras and L. Jiang, *Green Chem.*, 2019, **21**, 6579.
143 L. Hou, N. Wang, X. Man, Z. Cui, J. Wu, J. Liu, S. Li, Y. Gao, D. Li, L. Jiang and Y. Zhao, *ACS Nano*, 2019, **13**, 4124–4132.
144 X. Zhang, C. Liu, L. Zhang, L. Jia, M. Shi, L. Chen, Y. Di and Z. Gan, *Adv. Funct. Mater.*, 2021, **31**, 2010406.
145 Y. Zhao, C. Yu, H. Lan, M. Cao and L. Jiang, *Adv. Funct. Mater.*, 2017, **27**, 1701466.
146 Z. Wu, K. Yin, J. Wu, Z. Zhu, J. A. Duan and J. He, *Nanoscale*, 2021, **13**, 2209–2226.
147 B. Dai, K. Li, L. Shi, X. Wan, X. Liu, F. Zhang, L. Jiang and S. Wang, *Adv. Mater.*, 2019, **31**, 1904113.
148 X. He, S. Yang, Q. Pei, Y. Song, C. Liu, T. Xu and X. Zhang, *ACS Sens.*, 2020, **5**, 1548.

© 2022 The Author(s). Published by the Royal Society of Chemistry